Drug Design, Development and Therapy

Dovepress

open access to scientific and medical research

Open Access Full Text Article

ORIGINAL RESEARCH

Cell-Penetrating Peptide-Modified Graphene Oxide Nanoparticles Loaded with Rictor siRNA for the Treatment of Triple-Negative Breast Cancer

Yun-Yun Yang[1]
Wei Zhang[2]
Hui Liu[2]
Jun-Jie Jiang[2]
Wen-Jie Wang[3]
Zheng-Yan Jia[4]

[1]Outpatient Comprehensive Treatment, Cangzhou Central Hospital, Cangzhou, Hebei Province, People's Republic of China; [2]Department of Thyroid and Breast I, Cangzhou Central Hospital, Cangzhou, Hebei Province, People's Republic of China; [3]Department of General Surgery, Botou Hospital, Cangzhou, Hebei Province, People's Republic of China; [4]Department of General Surgery, Qingxian People's Hospital, Cangzhou, Hebei Province, People's Republic of China

Introduction: Breast cancer is a malignant tumor that seriously threatens women's life and health.

Methods: In this study, we proposed to use graphene nanoparticles loaded with siRNA that can silence Rictor molecules essential for the mammalian target of rapamycin (mTOR) complex 2 (mTORC2) complex to enhance gene delivery to tumor cells through modification of cell-penetrating peptide (CPP) for the treatment of breast cancer.

Results: Remarkably, we successfully synthesized graphene oxide (GO)/polyethyleneimine (PEI)/polyethylene glycol (PEG)/CPP/small interfering RNA (siRNA) system, and the results were observed by atomic force microscopy (AFM) and ultraviolet visible (UV-Vis) absorption spectra. The optimum mass ratio of siRNA to GO-PEI-PEG-CPP was 1:0.5. We screened out Rictor siRNA-2 from 9 candidates, which presented the highest inhibition rate, and this siRNA was selected for the subsequent experiments. We validated that Rictor siRNA-2 significantly reduced the Rictor expression in triple negative breast cancer (TNBC) cells. Confocal fluorescence microscope and flow cytometry analysis showed that GO-PEI-PEG-CPP/siRNA was able to be effectively uptake by TNBC cells. GO-PEI-PEG-CPP/siRNA improved the effect of siRNA on the inhibition of TNBC cell viability and the induction of TNBC cell apoptosis. The expression of Rictor and the phosphorylation of Akt and p70s6k were inhibited by GO-PEI-PEG-CPP/siRNA. Tumorigenicity analysis in nude mice showed that GO-PEI-PEG-CPP/siRNA significantly repressed the tumor growth of TNBC cells in vivo. The levels of ki-67 were repressed by GO-PEI-PEG-CPP/siRNA, and the apoptosis was induced by GO-PEI-PEG-CPP/siRNA in the system.

Discussion: Therefore, we concluded that CPP-modified GO nanoparticles loaded with Rictor siRNA significantly repressed TNBC progression by the inhibition of PI3K/Akt/mTOR signaling. Our finding provides a promising therapeutic strategy for the treatment of TNBC.

Keywords: triple-negative breast cancer, graphene oxide, cell-penetrating peptide, Rictor, PI3K/Akt/mTOR signaling

Introduction

Breast cancer is the top three causes of cancer-related death globally, particularly among gynecological cancers, with a high incidence and frequent metastasis.[1] Current clinical therapy for breast cancer mainly includes surgical operation, HER2-targeting therapy, endocrine therapy, as well as chemotherapy.[2] However,

Correspondence: Wei Zhang
Department of Thyroid and Breast I, Cangzhou Central Hospital, Cangzhou, Hebei Province, People's Republic of China
Email weiesiz685125@163.com

Received: 18 July 2021
Accepted: 1 October 2021
Published: 10 December 2021

conventional therapeutic strategies are limited to nonspecific targeting, poor biocompatibility and bioavailability, fast clearance in blood and so on.[2] Over the past several decades, gene targeting therapies, such as RNA interference, are widely investigated in cancer research area.[3] Small interfering RNA (siRNA) is capable of effectively silencing gene expression with a short sequence and holds highly targeting ability.[3] However, the naked siRNAs are vulnerable in the physiological environment, such as blood system, digestive system and intracellular lysosomes, and hence are easily degraded.[4] Therefore, the development of safe and effective delivery systems is urgent and the primary challenge for gene therapy. Viral vectors have been widely applied as drug delivery manner and advanced the gene therapy area, yet its application was limited to the immune reaction and potential recombination with other viruses.[5] On the other hand, the non-viral delivery method has showed great potential for drug delivery, characterized by the flexible structure and low immunogenicity.[6]

Over the past decades, the development of nanoparticles has provided promising delivery strategies for treatment of various cancers, including the TNBC. For example, the polymeric nanoparticles have been studied for the delivery of bioactive drugs either in pharmaceutical or biotechnological field, owing to their advantages to enhance the aqueous solubility of lipophilic drugs, control its release and increase the bioavailability of different drugs.[7–9] Besides, polymersome (PS)-based cancer nanomedicine effectively delivered the guanabenz acetate (GA) to TNBC cells, and caused a significant decrease in tumor size and weight compared to free GA.[10] Here, in this work, we designed and testified a novel graphene oxide (GO)-based delivery vector for breast cancer treatment.

GO, the derivative of graphite, has recently generated great attention in biological area, owing to its unique mechanical, electrical and thermal features.[11] The functional groups, including hydroxyls, epoxides, and carbonyls, on the surface of GO enable its chemical and biological properties, and subsequently its flexible modification, remarkable biocompatibility, which facilitates its advantage as an ideal delivery vector to load small molecular drugs, proteins, as well as nucleic acid sequences including DNA and RNA.[11] Studies indicated that degradation of thin GO sheets by normal mammalian tissue did not cause any detectable pathological consequences.[12] Moreover, the NO-dependent degradation of GO led to reduced inflammation in the gastrointestinal tract.[13] GO derivatives have been widely studied in drug and gene delivery for cancer therapy, due to their excellent capacity to condense materials, protect DNA and RNA from degradation caused by enzymes, and promote cellular internalization.[14]

Mammalian target of rapamycin (mTOR) is the critical participant in PI3K/AKT cell signaling transduction, which is closely related with cell growth, metastasis and therapy resistance of multiple cancers.[15–18] MTOR functions through forming to forms of complex, one of which contains Rictor and is indicated to regulate the phosphorylation and activation of AKT signaling.[19] Studies have suggested the critical role of Rictor during multiple processes of breast cancer development, such as cell growth, cell metabolism and protein expression.[20,21] Moreover, it has been reported that nanoparticle-based Rictor ablation successfully decreased the activation of Akt in HER2-amplified breast tumors and effectively caused tumor cell death.[22] Hence, targeting Rictor is a promising strategy for clinical therapy of cancers, including breast cancer.

In this work, we aimed to explore a novel GO-based siRNA delivery system for targeting Rictor and improve the clinical therapy for breast cancer. We obtained a GO-PEI-PEG-CPP vector which contains the polyethyleneimine (PEI) and polyethylene glycol (PEG) which facilitate the loading and delivery capacity, and a cell penetrating peptide (CPP) which enhances the cellular uptake and targeting ability of the vector. Furthermore, the in vitro and in vivo studies testified the effective inhibitory function of GO-PEI-PEG-CPP/siRNA in breast cancer. Our study provided a promising delivery system for breast cancer therapy.

Materials and Methods

Materials

The TNBC cell line MDA-MB-231 was obtained from American Type Cell Culture (ATCC, USA), cultured in a Dulbecco's modified eagle's medium (DMEM, Hyclone) supplied with fetal bovine serum (FBS, Gibco) and 1% penicillin and streptomycin (Sigma), placed in a 37°C humidified incubator filled with 5% CO_2. The graphene oxide (GO) was synthesized following the Hummer's method.[23] The polyethyleneimine (PEI, MW=800), polyethylene glycol (PEG, MW=2000) and Cy5 were purchased from Sigma (USA). The CPP Octaarginine (R8) (sequenced H-Arg-Arg-Arg-Unk-Arg-Arg-Arg-Arg-OH and weighted 1267 g/mol) used in this work was purchased from (PopChem, China). All siRNAs targeting Rictor (siRictor) and the scramble negative control (siScr) were designed and purchased from Qiagen (USA). Cy5 labeled siRictor was synthesized by conjugating cy5 to the 5′ region of siRictor and purchased from Santa Cruz, USA.

RNA Transfection and Quantification

To evaluate the efficacy of purchased siRNAs, cell transfection and RNA quantification experiments were performed. In brief, cells were transfected with siRictors by using a lipofectamine 2000 (Invitrogen, USA) under the manufacturer's instruction. After 24 hours, the cells were lysed by a Trizol reagent (Thermo) to extract RNAs. The cDNA was obtained from total RNA by using a SuperScript IV reverse transcription kit (Thermo) and quantified by a PowerUp SYBR™ Green reagent (Thermo). The relative expression of Rictor was normalized to GAPDH and calculated with the $2^{-\Delta\Delta Ct}$ method. The primers were as follows: Rictor, sense, 5′-TCCAAAGACTCGACAGTATGTGC-3′, antisense, 5′-GGCTAGAAATCGTGCTTCTCTG-3′; GAPDH, sense, 5′-TGTGGGCATCAATGGATTTGG-3′, antisense, 5′-ACAC CATGTATTCCGGGTCAAT-3′.

Instrumentation

The size and morphology of GO was observed and captured by an atomic force microscope (AFM, Nanoscope III, Germany). The absorbance curve of GO suspended in the MilliQ was detected by an UV–vis spectrophotometer (UV-EV 300, USA) in the range of 200 nm to 600 nm. The surface zeta potential and average particle size of the nanocomplexes at water solution were measured by dynamic light scattering (DLS, Malvern Zetasizer Nano ZS, UK).

GO Functionalization

The synthesis of GO-PEI-PEG-CPP follows the process below: At first, the GO suspension (1mg/mL, 5mL) was sonicated for 2 hours (50 W); then, the PEI was dropped in, followed by sonication constantly for 30 minutes and stirring for 12 hours at 4°C. To remove the excessed non-reacted reagent, the solution was subjected to dialysis with a membrane of MWCO 3500 Da (Thermo) for 24 hours. The addition of PEG followed the same process as PEI. The complexes were lyophilized. Subsequently, the CPP solution was added into the GO-PEI-PEG solution at a final concentration of 1 mM, and the mixture was sonicated for 1 h, then washed.

Agarose Gel Electrophoresis Mobility Assay

The siRNA/GO complexation at mass ratios of 1:0, 1:0.5, 1:1, 1:2, 1:3, 1:4, 1:5, 1:6, 1:8, 1:12, 1:16, 1:20 and 1:24, which contain an equivalent 200 ng siRNA, was loaded in vehicles of different GO/PEI mass ratios (1:10, 1:20, 1:40, 1:60, 1:80, and 1:100), and was left to set for 20 min at room temperature. The acquired samples were subjected to electrophoresis in a 2% agarose gel containing DNA loading dye (6X, SolarBio, China), in 0.5x Tris-Acetate-EDTA (TAE) buffer, and run for 30 minutes at 100 mV. The visualization of bands was achieved in a UV Gel Imaging system (BioRad, USA).

Generation of GO:siRNA Complexes

GO:siRNA complexes were obtained by simple pipetting of siRNA with different amounts of GO to achieve the following final GO:siRNA mass ratios: 0.5:1, 1:1, 2:1, 3:1, 4:1, 5:1, 6:1, 8:1, 12:1, 16:1, 20:1, and 24:1. Complexes were left to form for 30 min at room temperature prior to their characterization or use for siRNA transfection studies.

Stability Assessment

The stability of GO-PEI-PEG-CPP in phosphate buffer saline (PBS) and cell culturing medium was assessed. Briefly, the complexes at different GO/PEI mass ratios (1:10, 1:20, 1:40. 1:60, 1:80, and 1:100) were dispersed in PBS or DMEM containing 10% FBS, incubated at room temperature and stand for three months. The solution status was observed and photographed.

The stability of siRNA/GO complexation in physical condition was measured by agarose gel electrophoresis. In brief, free siRNA and siRNA/GO complexation were suspended in 50% human serum, incubated at 37°C for 0, 3, 6, 24, 48, 72 hours, followed by separation in a 2% agarose gel to detect the level of siRNA.

Cell Uptake Study

To determine the uptake of nanocomplexes into cells, we adopted fluorescence microscope and flow cytometry to assess the fluorescence intensity. In brief, MDA-MB-231 cells were placed in a confocal dish (10^5 cells) and cultured 24 hours. Then, the cy5 labeled siRNA (cy5-siRNA) as control, and the complexes of cy5-siRNA packaged by GO-PEI-PEG or GO-PEI-PEG-CPP were added. After incubation for 24 hours, the cells were fixed in 4% paraformaldehyde and stained with a DAPI reagent (0.5 g/mL, Thermo). The fluorescence of cy5 was observed and captured under 633 nm exciter by a microscope (Carl Zeiss, Germany). For flow cytometry, the cells were treated with indicated nanocomplexes for 24 hours, collected, suspended in PBS (10^7/mL), and the fluorescence intensity was evaluated by the flow cytometer (BD Biosciences, USA) under excitation of 633 nm.

Release Study

The release behaviour of FITC tagged siRNA from the three- and five-layered particles was observed in PBS over a span of 14 days. Three-layered LbL particles and five-layered LbL particles fabricated with 1 mg HA, respectively, were dispersed in 600 μL of PBS and incubated at 37°C with constant shaking over 14 days. The doses of particles were disassembled by overnight treatment of trypsin to find the total siRNA contents after measurements with the Tecan plate reader. At the stipulated time points, the particle samples were centrifuged down and the supernatant collected and measured with the Tecan plate reader to affirm release amount compared against a series of FITC siRNA standard curve (Tecan readings taken from FITC siRNA of known concentrations). Fresh PBS was added for subsequent time point measurements. All samples and measurements were conducted in triplicates.

Cellular Cytotoxicity

The cellular cytotoxicity was assessed by MTT, colony formation, and apoptosis assays. For MTT assay, 5000 MDA-MB-231 cells were placed in each well of a 96-well plate, followed by administration of GO-PEI-PEG /siRNA, GO-PEI-PEG-CPP/siRNA, or siRNA as control, at densities of 0, 50, 100, and 150 nM. After 24 hours incubation, 10 μL MTT solution was added in the medium to incubate for another 4 hours, followed by replacement with 150 μL DMSO. The absorbance at 490 nm was detected by a microplate reader.

For colony formation assay, MDA-MB-231 cells were suspended as single cell and seeded into a 6-well plate with 1000 cells per well, and incubated for 2 weeks to form visible colonies. The colonies were stained by 1% crystal violate resolved in methanol for 30 minutes and photographed.

To determine apoptotic cells, we adopted an Annexin-V/PI apoptosis detection kit (Thermo). In short, 5×10^5 MDA-MB-231 cells were placed in each well of a 6-well plate, treated with indicated nanocomplexes, digested, and suspended in binding buffer. Subsequently, the cells were stained by Annexin-V for 20 minutes at room temperature, followed by staining with PI. The samples were analyzed on a C6 flow cytometer (BD Biosciences, USA).

Western Blotting

Total protein was extracted from MDA-MB-231 cells treated with indicated nanocomplexes using a RIPA lysis reagent (Beyotime, China), quantified by using a BCA kit (Beyotime), separated in the SDS-PAGE gel and transferred to PVDF membranes. Subsequently, the blots were soaked in blocking buffer for 15 minutes, and incubated in diluted primary antibodies against Rictor (ab105469), Akt (ab8805), phosphorylated-Akt (ab38449), p70s6k (ab32359), phosphorylated p70s6k (ab59208), and tubulin (ab7291) as internal control, overnight at 4°C. Next day, the blots were washed with PBS and incubated with HRP-conjugated secondary anti-mouse or anti-rabbit antibody, accordingly. All antibodies used in this work were purchased from Abcam (USA) and diluted as instructions of the manufacturer. The blots were visualized by using the ECL solution (Invitrogen) and captured in a gel imaging system (BioRad).

Mice Model and Immunohistochemistry (IHC)

SCID/nude mice (n = 24) aged 5-week were obtained from Vital River (China). MDA-MB-231 cells (1×10^6, 100μL) were mixed with Matrigel (BD Biosciences) at 1:1 and subcutaneously injected into the left fat pad of SCID/nude mice (5-week aged, Vital River, China), and the mice were randomly divided into four groups for administration of different nanocomplexes. Two weeks after inoculation, siRNA, GO-PEI-PEG/siRNA or GO-PEI-PEG-CPP/siRNA were injected through tail vein, and saline was used in the control group. The tumor size and body weight were measured once in three days for 18 days. After that, the tumors were isolated, fixed, and paraffin-embedded to obtain tissue sections. The tissue sections were subjected to Ki-67 and tunnel staining following manufacturer's protocol. This study was carried out in accordance with the recommendations in the Guide for the Care and Use of Laboratory Animals of the National Institutes of Health. All animal experiments were authorized by the Animal Research Committee of Cangzhou Central Hospital and have followed internationally recognized guidelines, ARRIVE guidelines.

Statistics

Each experiment was repeated three times, and the data was presented as means ± SD. Statistical analysis was carried out by using a GraphPad prism (ver.17.0). Student's *t*-test and one-way ANOVA were adopted to evaluate differences between two or more groups. Differences with $P<0.05$ was regarded as statistically significant.

Results

GO and GO-PEI-PEG-CPP Preparation and Characterization

Firstly, graphene oxide (GO) was successfully synthesized. The GO sheets presented layered and smooth in the formation of lyophilization and preparation, and the particle morphology sheet-like morphology with the size from 0.06 to 2 μm was detected by atomic force microscopy (AFM) (Figure 1A). The GO formation was further confirmed by the UV-Vis absorption spectra, manifested by peak GO at 230nm (Figure 1B). Moreover, the stability of GO-PEI-PEG-CPP in PBS and DMEM within 24 hours and 3 months was validated (Figure 1C).

Screening of the siRNA Delivery System

The binding ability of GO-PEI-PEG-CPP complex with siRNA was detected by agarose gel electrophoresis. When siRNA binds to GO-PEI-PEG-CPP complex, the band will be significantly darker than that of siRNA alone, and when the bright band disappears, it means that GO-PEI-PEG-CPP can bind siRNA completely. As shown in Figure 2A, when the GO:PEI ratio is 1:10, 1:20 and 1:40, the siRNA binds completely with the mass ratio of GO-PEI-PEG-CPP at 1:24, 1:20, 1:12; when the GO:PEI ratio is 1:60, 1:80 and 1:100, the binding of siRNA to GO-PEI-PEG-CPP was complete at the mass ratio of 1:0.5, respectively. The stronger the ability of GO-PEI-PEG-CPP to bind the plasmid, the less the material used and the lower the cost. The optimum mass ratio of siRNA to GO-PEI-PEG-CPP was 1:0.5 (Figure 2A). Then, screened siRNAs of Rictor from 9 candidates, in which Rictor siRNA-2 presented the most efficient with a 70% inhibition rate, and this siRNA was selected for the subsequent experiments to confirm that this siRNA could effectively inhibit mTOR expression (Figure 2B). We validated the efficiency of Rictor siRNA-2, and we found that Rictor siRNA-2 significantly

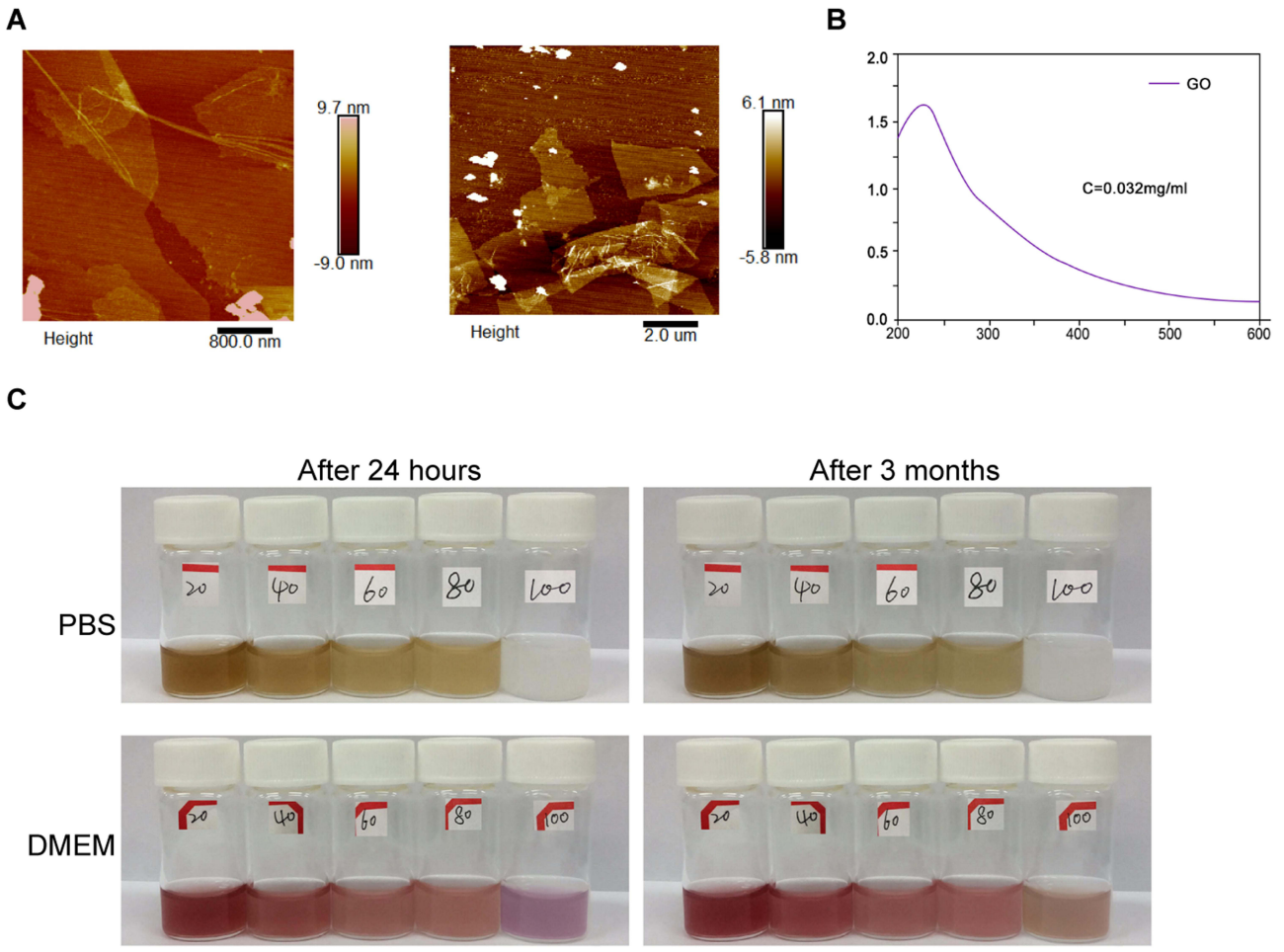

Figure 1 GO and GO-PEI-PEG-CPP preparation and Characterization. (**A**) The representative AFM images of GO were demonstrated. (**B**) The UV-Vis absorption spectra of GO were shown. (**C**) The stability of GO-PEI-PEG-CPP was analyzed.

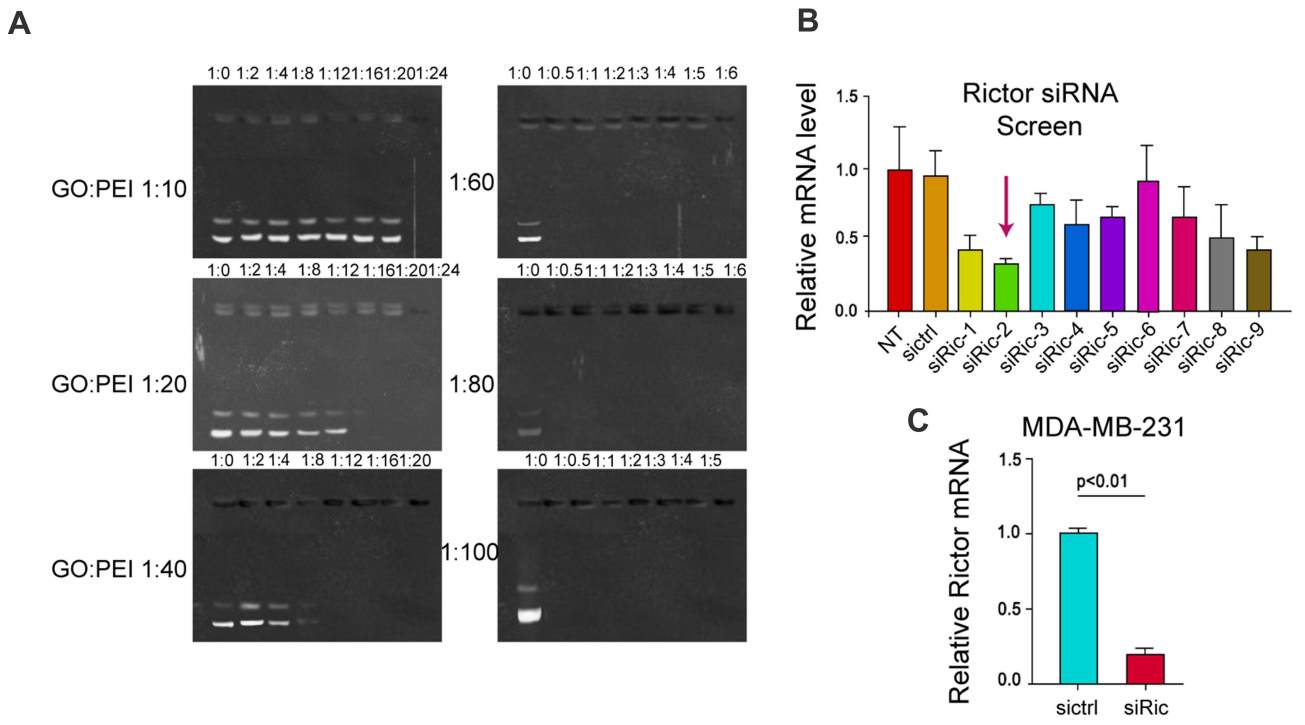

Figure 2 Screening of the siRNA that targets Rictor. (**A**) The 1% agarose gel electrophoresis was applied to screen and compare the effect of different ratios of GO and PEI in GO-PEI-PEG-CPP/siRNA complexes on the ability to bind siRNA. (**B**) The expression of Rictor was analyzed by qPCR in the cells treated with the Rictor siRNAs. (**C**) The expression of Rictor was detected by qPCR in the cells treated with control siRNA or Rictor siRNA-2.

reduced the Rictor expression in MDA-MB-231 cells (Figure 2C). According to the results from DLS and AFM, the particle size (~200 nm) and morphology of GO-PEI-PEG-CPP/siRNA at 0 and 24 hours did not change, suggested the stability of materials (Figure S1A and B). Moreover, we assessed the stability of the GO-PEI-PEG-CPP/siRNA in serum. As shown in Figure S1C, the siRNA encapsulated in GO-PEI-PEG-CPP nanoparticles showed notably higher stability than the naked siRNA, especially after 12 hours. These data determined the successful preparation of GO-PEI-PEG-CPP/siRNA delivery system and its stability.

The Cellular Uptake of GO-PEI-PEG-CPP /siRNA

To determine the effect of GO-PEI-PEG-CPP/siRNA on TNBC cells, we first assessed the release of siRNA from GO-PEI-PEG-CPP. As shown in Figure 3A, the siRNA could be effectively released by GO-PEI-PEG-CPP within two weeks. Next, the cellular uptake of GO-PEI-PEG-CPP /siRNA was analyzed by confocal fluorescence microscope and flow cytometry in MDA-MB-231 cells. The Cy5-labeled siRNA was notably presented in the plasma of breast cancer cells when delivered by the GO-PEI-PEG-CPP, in comparison with the pure siRNAs or GO-PEI-PEG group (Figure 3B and C). Moreover, we evaluated the zeta potential of the synthesized nanomaterials, and found that the GO-PEI-PEG-CPP/siRNA presented a positive charge (16.1 ± 1.057) comparing with the GO material, suggesting its ability to penetrate the cell membrane (Table 1). Our data showed that GO-PEI-PEG-CPP/siRNA was able to be effectively uptake by MDA-MB-231 cells (Figure 3A and B).

The Effect of GO-PEI-PEG-CPP/siRNA on Breast Cancer Cell Proliferation and Apoptosis in vitro

Next, we found that GO-PEI-PEG/siRNA reduced the MDA-MB-231 cell viability and GO-PEI-PEG-CPP/siRNA further enhanced the effect in the cells, with IC50 values around 150 nM and 100 nM, respectively (Figure 4A). The colony formation numbers of MDA-MB-231 cells were repressed by GO-PEI-PEG-CPP/siRNA (Figure 4B). The treatment of GO-PEI-PEG-CPP/siRNA induced MDA-MB -231 cell apoptosis (Figure 4C). Meanwhile, our data showed that the expression of Rictor, and the phosphorylation of Akt and p70s6k was inhibited by GO-PEI-PEG

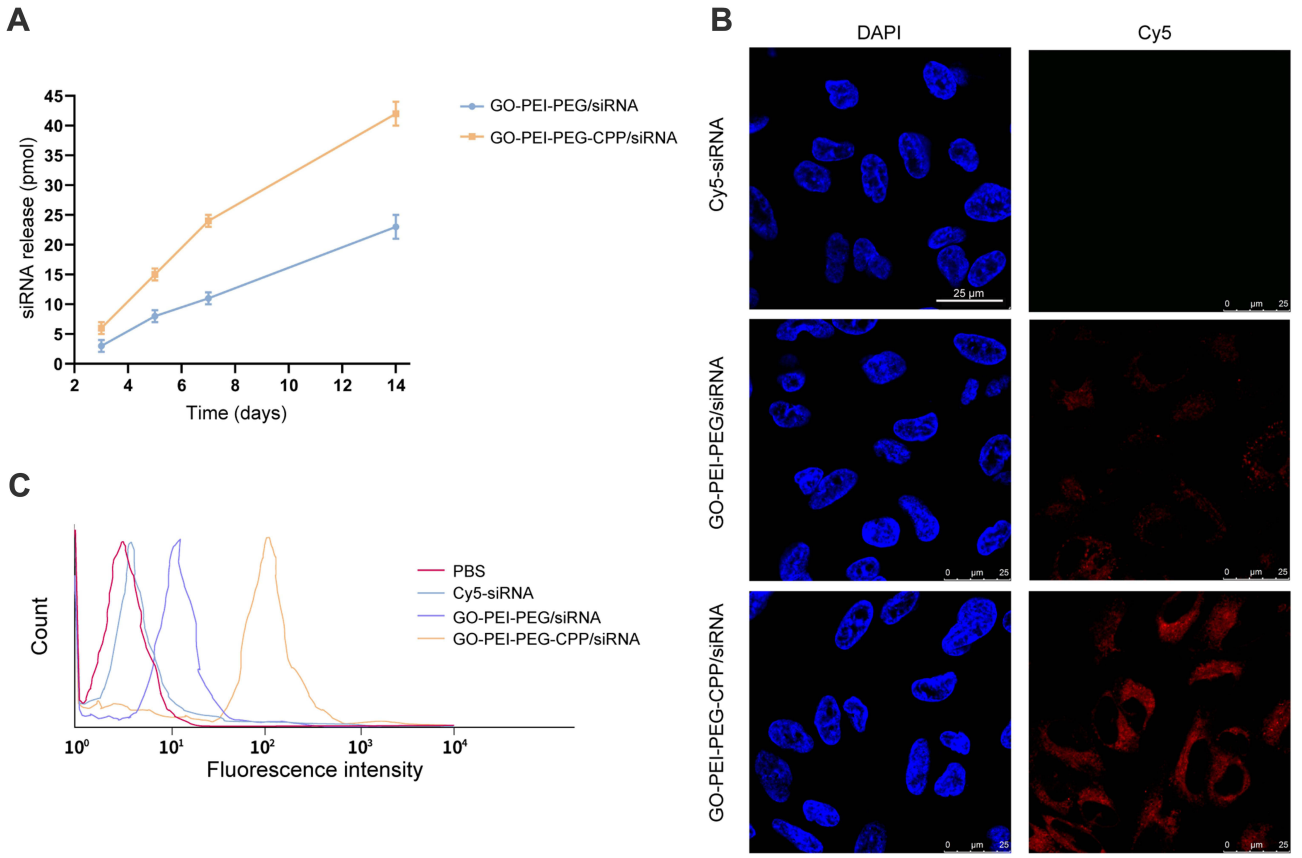

Figure 3 The intracellular uptake of GO-PEI-PEG-CPP/siRNA by TNBC cells. (**A**–**C**) The cellular uptake of GO-PEI-PEG-CPP/siRNA was analyzed by confocal fluorescence microscope and flow cytometry in MDA-MB-231 cells.

/siRNA, while GO-PEI-PEG-CPP/siRNA further reinforced the inhibition in MDA-MB-231 cells (Figures 4D and S2).

The Effect of GO-PEI-PEG-CPP/siRNA on Breast Cancer Cell Growth in vivo

Next, we evaluated the effect of GO-PEI-PEG-CPP /siRNA on breast cancer cell growth in vivo. Tumorigenicity analysis in nude mice showed that the administration of siRNA, GO-PEI-PEG/siRNA and GO-PEI-PEG-CPP/siRNA did not affect the body weight of the mice, comparing with the control group (Figure 5A). GO-PEI-PEG/siRNA reduced the tumor volume, tumor weight, and tumor size in the nude mice (Figure 5B–D), while GO-PEI-PEG-CPP/siRNA further enhanced the reduction effect on the tumor growth (Figure 5B–D). Meanwhile, the levels of ki-67 were repressed by GO-PEI-PEG-CPP/siRNA, and the apoptosis was induced by GO-PEI-PEG-CPP/siRNA in the system (Figure 5E).

Table 1 Zeta Potential of Nanomaterials

Materials	Size (nm)	Zeta (mV)
GO	195.2±2.185	−30.6±3.031
GO-PEI-PEG-CPP	229.4±2.402	16.4±1.294
GO-PEI-PEG-CPP/siRNA	231.6±3.261	16.1±1.057

Discussion

TNBC is the most aggressive subtype of breast cancer that seriously threatens women's health. The usage of nanomaterials for cancer treatment has been a popular research focus over the past decade. For example, the poly(ethylene glycol)-poly(e-caprolactone) (PEG-PCL) polymersomes could effectively deliver therapeutic drugs including the artemisinin and methotrexate to cancer cells to facilitate cytotoxicity[24,25] ["DOI:10.1016/j.eurpolymj.2018.04.020" and "DOI:10.1021/acsbiomaterials.8b01420"]. Among the various nanomaterials, GO has presented significant biocompatibility and stability in aqueous solution. In this study, we applied a GO-PEI-PEG-CPP system which contains the PEI and PEG, which facilitated the loading and delivery capacity, and CPP, which enhanced the cellular

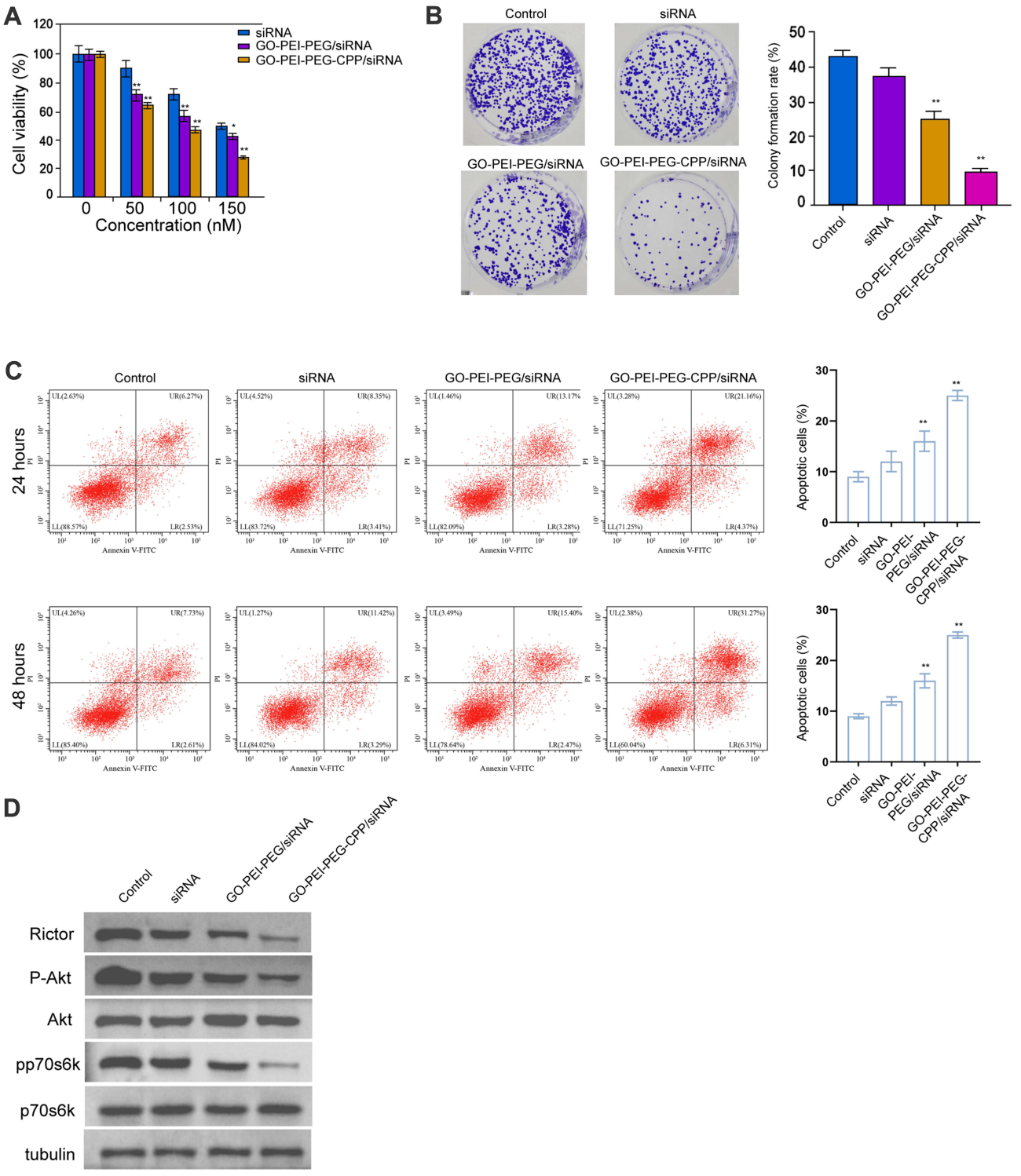

Figure 4 The effect of GO-PEI-PEG-CPP/siRNA on breast cancer cell proliferation and apoptosis in vitro. (**A**–**D**) The MDA-MB-231 cells were treated with siRNA, GO-PEI-PEG/siRNA, or GO-PEI-PEG-CPP/siRNA. (**A**) The cell viability was analyzed by MTT assays. (**B**) The cell proliferation was measured by colony formation assays. (**C**) The cell apoptosis was detected by Annexin-V/PI apoptosis detection kit. Histogram showed the portion of apoptotic cells. (**D**) The expression of Rictor, Akt, p70s6k, and the phosphorylation of Akt and p70s6k were determined by Western blot analysis. Data are presented as mean ± SD. Statistic significant differences were indicated: **P*<0.05, ***P* < 0.01.

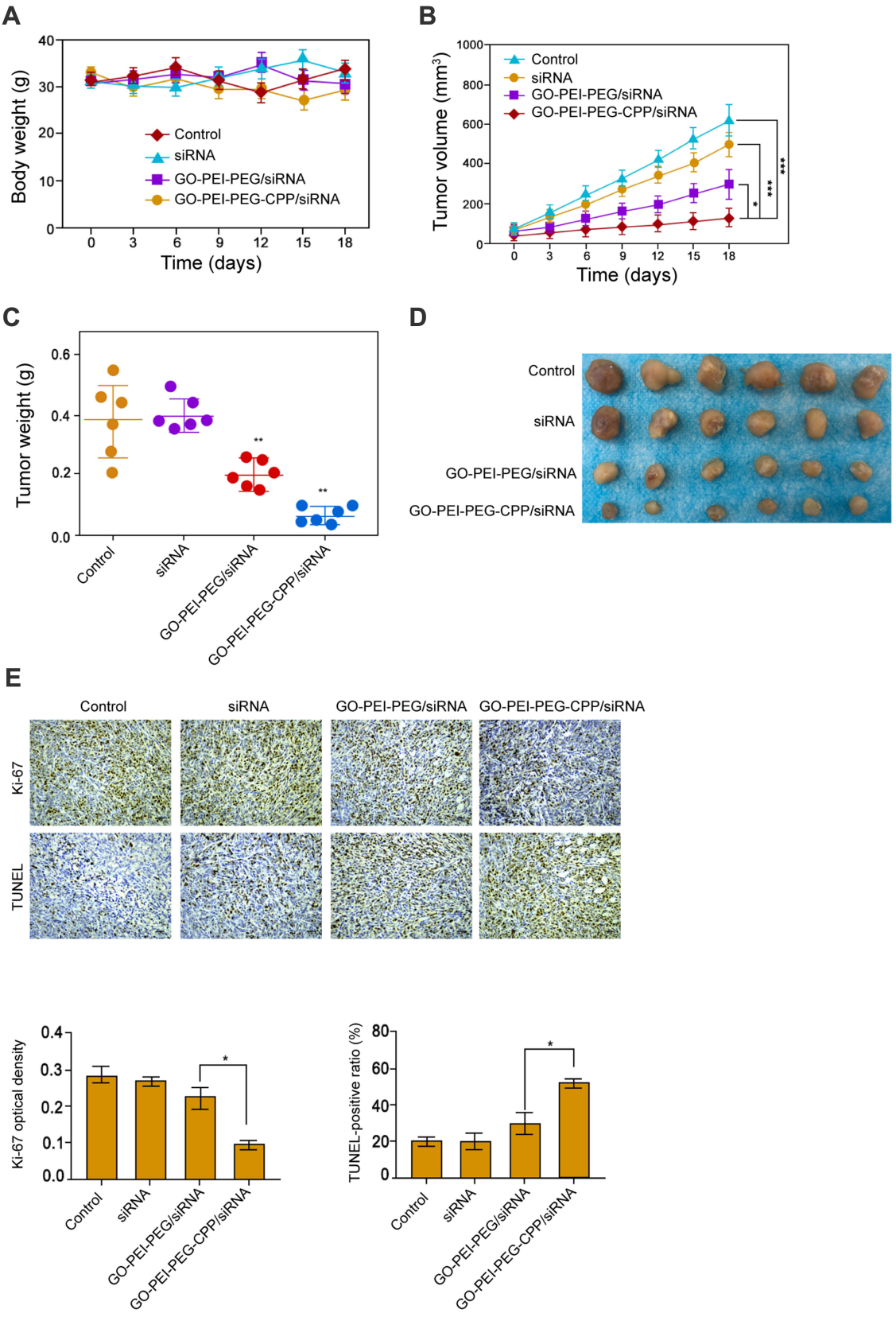

Figure 5 The effect of GO-PEI-PEG-CPP/siRNA on breast cancer cell growth in vivo. (**A-E**) The nude mice were injected with MDA-MB-231 cells and were treated with siRNA, GO-PEI-PEG/siRNA, or GO-PEI-PEG-CPP/siRNA. (**A**) The body weight was remarketed. (**B**) The tumor volume was shown. (**C**) The tumor weight was shown. (**D**) The tumor size was shown. (**E**) The level of ki-67 was measured by IHC and apoptosis was analyzed by TUNEL staining (10 x objective). Data are presented as mean ± SD. Statistic significant differences were indicated: $^{*}P < 0.05$, $^{**}P < 0.01$, $^{***}P < 0.001$.

https://doi.org/10.2147/DDDT.S330059

uptake and targeting ability. We identified that GO-PEI-PEG-CPP/siRNA demonstrated remarkable inhibitory effect on TNBC in vitro and in vivo.

GO, PEI, and CPP are widely applied in drug delivery for the cancer treatment. It has been reported that GO-chitosan[22] -CPP-miR33a/miR199a drug-delivery system is successfully established and represses melanoma progression.[26] PEG-GO -PEI- folic acid (FA)/siRNA may provide a potential therapeutic strategy for siRNA delivery for folate receptor (FR)-related ovarian cancer.[27] The combination of Photothermal and Genetherapy with siRNA delivery with PEGylated GO/siRNA delivery complex inhibits pancreatic cancer development.[28] Anti-HER2 functionalized GO serves as survivin siRNAs-delivery system and reduces breast cancer progression in vivo and in vitro.[29] Functional GO with Stat3 siRNA decreases mouse melanoma cell growth in -vivo.[30] Plasmid-based Stat3 siRNA loaded by functional GO inhibits melanoma progression in mouse model.[31] Meanwhile, it has been reported that Rictor contributes to rapamycin-insensitive TNBC progression.[32] Previous studies have demonstrated that Rictor/mTORC2 promotes therapeutic resistance and progression of HER2-amplified breast cancer,[33] and selective mTORC2 inhibition therapeutically represses cell survival and growth of breast cancer.[22] In this study, we successfully constructed a GO/PEI/PEG/CPP/siRNA with Rictor siRNA. The characterization experiments indicated the particle size around 200 nm and the positive zeta potential of GO/PEI/PEG/CPP/siRNA, which suggested its stability and ability to penetrate into cells. Further confocal fluorescence microscope and flow cytometry analysis showed that GO-PEI-PEG-CPP/siRNA was able to be effectively uptaken by TNBC cells. It indicates a novel delivery system of Rictor siRNA. Meanwhile, in vitro experiments demonstrated that GO-PEI-PEG-CPP/siRNA improved the effect of siRNA on the inhibition of TNBC cell viability and the induction of TNBC cell apoptosis. The expression of Rictor and the phosphorylation of Akt and p70s6k were inhibited by GO-PEI-PEG-CPP/siRNA. In vivo xenograft model in nude mice showed that GO-PEI-PEG-CPP/siRNA significantly repressed the tumor growth of TNBC cells in comparison with the GO-PEI-PEG /siRNA group and siRNA group. The levels of ki-67 were repressed by GO-PEI-PEG-CPP/siRNA, and the apoptosis was induced by GO-PEI-PEG -CPP/siRNA in the system. These results were consistent with the published works showing that repression of mTORC2 suppressed breast cancer progression. Our data suggest that GO-PEI-PEG-CPP/siRNA could significantly improve the delivery and uptake effectiveness of Rictor siRNA for the treatment of TNBC.

CPP has been widely applied as a powerful tool for both fundamental biology and medical applications. They are capable of transporting nucleic acids including siRNAs, plasmids, antisense oligomers, and decoy DNA, for which intracellular delivery is often limited by high molecular weight and negative charges, making the modulation of gene expression easier[34] [DOI: 10.1007/s10853-017-1673-6]. Nowadays, more than 25 CPP-conjugated drugs are under clinical development for therapy of inflammation, pain, cancer, heart diseases, and aging.[35–39] In our work, we suggested that the siRNA delivery system that linked with CPP showed stronger ability to penetrate into breast cancer cells and exhibited higher cytotoxicity both in vitro and in vivo.

Conclusion

To summarize, we synthesized a CPP-modified GO nanoparticles to successfully deliver the Rictor siRNA, which notably repressed TNBC progression by inhibiting the PI3K/Akt/mTOR signaling. Our findings may provide a promising therapeutic strategy for the gene therapy of TNBC.

Disclosure

The authors declare no competing interests.

References

1. Siegel RL, Miller KD, Jemal A. Cancer statistics, 2020. *CA Cancer J Clin*. 2020;70(1):7–30. doi:10.3322/caac.21590
2. Harbeck N, Gnant M. Breast cancer. *Lancet*. 2017;389 (10074):1134–1150. doi:10.1016/S0140-6736(16)31891-8
3. Husain SR, Han J, Au P, Shannon K, Puri RK. Gene therapy for cancer: regulatory considerations for approval. *Cancer Gene Ther*. 2015;22(12):554–563. doi:10.1038/cgt.2015.58
4. Joo MK, Yhee JY, Kim SH, Kim K. The potential and advances in RNAi therapy: chemical and structural modifications of siRNA molecules and use of biocompatible nanocarriers. *J Control Release*. 2014;193:113–121. doi:10.1016/j.jconrel.2014.05.030
5. Thomas CE, Ehrhardt A, Kay MA. Progress and problems with the use of viral vectors for gene therapy. *Nat Rev Genet*. 2003;4(5):346–358. doi:10.1038/nrg1066
6. Yin H, Kanasty RL, Eltoukhy AA, Vegas AJ, Dorkin JR, Anderson DG. Non-viral vectors for gene-based therapy. *Nat Rev Genet*. 2014;15(8):541–555. doi:10.1038/nrg3763
7. Haggag Y, Abu Ras B, El-Tanani Y, et al. Co-delivery of a RanGTP inhibitory peptide and doxorubicin using dual-loaded liposomal carriers to combat chemotherapeutic resistance in breast cancer cells. *Expert Opin Drug Deliv*. 2020;17(11):1655–1669. doi:10.1080/17425247.2020.1813714
8. Haggag Y, Elshikh M, El-Tanani M, Bannat IM, McCarron P, Tambuwala MM. Nanoencapsulation of sophorolipids in PEGylated poly(lactide-co-glycolide) as a novel approach to target colon carcinoma in the murine model. *Drug Deliv Transl Res*. 2020;10 (5):1353–1366. doi:10.1007/s13346-020-00750-3

9. Haggag YA, Ibrahim RR, Hafiz AA. Design, formulation and in vivo evaluation of Novel Honokiol-loaded PEGylated PLGA nanocapsules for treatment of breast cancer. *Int J Nanomed*. 2020;15:1625–1642. doi:10.2147/IJN.S241428
10. Haggag YA, Yasser M, Tambuwala MM, El Tokhy SS, Isreb M, Donia AA. Repurposing of Guanabenz acetate by encapsulation into long-circulating nanopolymersomes for treatment of triple-negative breast cancer. *Int J Pharm*. 2021;600:120532. doi:10.1016/j.ijpharm.2021.120532
11. Goenka S, Sant V, Sant S. Graphene-based nanomaterials for drug delivery and tissue engineering. *J Control Release*. 2014;173:75–88. doi:10.1016/j.jconrel.2013.10.017
12. Newman L, Jasim DA, Prestat E, et al. Splenic capture and in vivo intracellular biodegradation of biological-grade graphene oxide sheets. *ACS Nano*. 2020;14(8):10168–10186. doi:10.1021/acsnano.0c03438
13. Peng G, Montenegro MF, Ntola CNM, et al. Nitric oxide-dependent biodegradation of graphene oxide reduces inflammation in the gastrointestinal tract. *Nanoscale*. 2020;12(32):16730–16737. doi:10.1039/D0NR03675G
14. Vincent M, de Lazaro I, Kostarelos K. Graphene materials as 2D non-viral gene transfer vector platforms. *Gene Ther*. 2017;24(3):123–132. doi:10.1038/gt.2016.79
15. Sadeghi N, Gerber DE. Targeting the PI3K pathway for cancer therapy. *Future Med Chem*. 2012;4(9):1153–1169. doi:10.4155/fmc.12.56
16. Hua H, Kong Q, Zhang H, Wang J, Luo T, Jiang Y. Targeting mTOR for cancer therapy. *J Hematol Oncol*. 2019;12:71.
17. Ippen FM, Grosch JK, Subramanian M, et al. Targeting the PI3K/Akt/mTOR pathway with the pan-Akt inhibitor GDC-0068 in PIK3CA-mutant breast cancer brain metastases. *Neuro Oncol*. 2019;21(11):1401–1411. doi:10.1093/neuonc/noz105
18. Sharma V, Sharma AK, Punj V, Priya P. Recent nanotechnological interventions targeting PI3K/Akt/mTOR pathway: a focus on breast cancer. *Semin Cancer Biol*. 2019;59:133–146. doi:10.1016/j.semcancer.2019.08.005
19. Sarbassov DD, Guertin DA, Ali SM, Sabatini DM. Phosphorylation and regulation of Akt/PKB by the Rictor-mTOR complex. *Science*. 2005;307(5712):1098–1101. doi:10.1126/science.1106148
20. Guertin DA, Stevens DM, Thoreen CC, et al. Ablation in mice of the mTORC components raptor, Rictor, or mLST8 reveals that mTORC2 is required for signaling to Akt-FOXO and PKCalpha, but not S6K1. *Dev Cell*. 2006;11(6):859–871. doi:10.1016/j.devcel.2006.10.007
21. Oh WJ, Jacinto E. mTOR complex 2 signaling and functions. *Cell Cycle*. 2011;10(14):2305–2316. doi:10.4161/cc.10.14.16586
22. Werfel TA, Wang S, Jackson MA, et al. Selective mTORC2 inhibitor therapeutically blocks breast cancer cell growth and survival. *Cancer Res*. 2018;78(7):1845–1858. doi:10.1158/0008-5472.CAN-17-2388
23. Morimoto N, Kubo T, Nishina Y. Tailoring the oxygen content of graphite and reduced graphene oxide for specific applications. *Sci Rep*. 2016;6(1):21715. doi:10.1038/srep21715
24. Nosrati H, Adinehvand R, Manjili HK, Rostamizadeh K, Danafar H. Synthesis, characterization, and kinetic release study of methotrexate loaded mPEG-PCL polymersomes for inhibition of MCF-7 breast cancer cell line. *Pharm Dev Technol*. 2019;24(1):89–98. doi:10.1080/10837450.2018.1425433
25. Nosrati H, Barzegari P, Danafar H, Kheiri Manjili H. Biotin-functionalized copolymeric PEG-PCL micelles for in vivo tumour-targeted delivery of artemisinin. *Artif Cells Nanomed Biotechnol*. 2019;47(1):104–114. doi:10.1080/21691401.2018.1543199
26. Liu C, Xie H, Yu J, et al. A targeted therapy for melanoma by graphene oxide composite with microRNA carrier. *Drug Des Devel Ther*. 2018;12:3095–3106. doi:10.2147/DDDT.S160088
27. Wang Y, Sun G, Gong Y, Zhang Y, Liang X, Yang L. Functionalized folate-modified graphene oxide/PEI siRNA nanocomplexes for targeted ovarian cancer gene therapy. *Nanoscale Res Lett*. 2020;15(1):57. doi:10.1186/s11671-020-3281-7
28. Yin F, Hu K, Chen Y, et al. SiRNA delivery with PEGylated graphene oxide nanosheets for combined photothermal and genetherapy for pancreatic cancer. *Theranostics*. 2017;7(5):1133–1148. doi:10.7150/thno.17841
29. Wang X, Sun Q, Cui C, Li J, Wang Y. Anti-HER2 functionalized graphene oxide as survivin-siRNA delivery carrier inhibits breast carcinoma growth in vitro and in vivo. *Drug Des Devel Ther*. 2018;12:2841–2855. doi:10.2147/DDDT.S169430
30. Yin D, Li Y, Lin H, et al. Functional graphene oxide as a plasmid-based Stat3 siRNA carrier inhibits mouse malignant melanoma growth in vivo. *Nanotechnology*. 2013;24(10):105102. doi:10.1088/0957-4484/24/10/105102
31. Yin D, Li Y, Guo B, et al. Plasmid-based Stat3 siRNA delivered by functional graphene oxide suppresses mouse malignant melanoma cell growth. *Oncol Res*. 2016;23(5):229–236. doi:10.3727/096504016X14550280421449
32. Watanabe R, Miyata M, Oneyama C. Rictor promotes tumor progression of rapamycin-insensitive triple-negative breast cancer cells. *Biochem Biophys Res Commun*. 2020;531(4):636–642. doi:10.1016/j.bbrc.2020.08.012
33. Morrison Joly M, Hicks DJ, Jones B, et al. Rictor/mTORC2 drives progression and therapeutic resistance of HER2-amplified breast cancers. *Cancer Res*. 2016;76(16):4752–4764. doi:10.1158/0008-5472.CAN-15-3393
34. Ramsey JD, Flynn NH. Cell-penetrating peptides transport therapeutics into cells. *Pharmacol Ther*. 2015;154:78–86. doi:10.1016/j.pharmthera.2015.07.003
35. Gurney LRI, Taggart J, Tong WC, Jones AT, Robson SC, Taggart MJ. Inhibition of inflammatory changes in human myometrial cells by cell penetrating peptide and small molecule inhibitors of NFkappaB. *Front Immunol*. 2018;9:2966. doi:10.3389/fimmu.2018.02966
36. Peng J, Rao Y, Yang X, et al. Targeting neuronal nitric oxide synthase by a cell penetrating peptide Tat-LK15/siRNA bioconjugate. *Neurosci Lett*. 2017;650:153–160. doi:10.1016/j.neulet.2017.04.045
37. Jia L, Gorman GS, Coward LU, et al. Preclinical pharmacokinetics, metabolism, and toxicity of azurin-p28 (NSC745104) a peptide inhibitor of p53 ubiquitination. *Cancer Chemother Pharmacol*. 2011;68(2):513–524. doi:10.1007/s00280-010-1518-3
38. Koutsokeras A, Purkayastha N, Rigby A, et al. Generation of an efficiently secreted, cell penetrating NF-kappaB inhibitor. *FASEB J*. 2014;28(1):373–381. doi:10.1096/fj.13-236570
39. Fu LS, Wu YR, Fang SL, et al. Cell penetrating peptide derived from human eosinophil cationic protein decreases airway allergic inflammation. *Sci Rep*. 2017;7(1):12352. doi:10.1038/s41598-017-12390-8